Arthritis Care & Research
Vol. 64, No. 11, November 2012, pp 1657–1664
DOI 10.1002/acr.21739

ORIGINAL ARTICLE

Novel Automated System for Magnetic Resonance Imaging Quantification of the Inflamed Synovial Membrane Volume in Patients With Juvenile Idiopathic Arthritis

C. MALATTIA,[1] M. B. DAMASIO,[2] C. BASSO,[3] M. SANTORO,[3] A. VERRI,[3] S. PEDERZOLI,[2] C. MATTIUZ,[2] S. VIOLA,[2] A. BUONCOMPAGNI,[2] A. MADEO,[2] M. MAZZONI,[2] K. ROSENDAHL,[4] K. LAMBOT-JUHAN,[5] L. TANTURRI DE HORATIO,[6] G. M. MAGNANO,[2] A. RAVELLI,[1] AND A. MARTINI[1]

Objective. **To introduce a novel automated method for the quantification of the inflamed synovial membrane volume (SV) using magnetic resonance imaging (MRI), and to investigate its feasibility and validity in patients with juvenile idiopathic arthritis (JIA).**

Methods. **The tool was tested on 58 patients with JIA and wrist involvement. Thirty-six patients had a 1-year MRI followup. MRI of the clinically more affected wrist was performed using a 1.5T scanner and a Flex small coil. An algorithmic approach, based on supervised voxel classification for automatic estimation of SV in a 3-dimensional MRI, was developed. The SV was estimated as the number of positively classified voxels and then normalized by the patient's body surface (NSV). Validation procedures included the analysis of reliability, construct validity, responsiveness to change, discriminant validity, and the predictive value.**

Results. **The agreement between the automated estimation of NSV and the manual measurements was excellent (intraclass correlation coefficient 0.93, 95% confidence interval 0.79–0.98). The automatic NSV demonstrated good construct validity by yielding strong correlations with local signs of disease activity and a moderate correlation with global physician assessment of disease activity and with the Rheumatoid Arthritis Magnetic Resonance Imaging Scoring system synovitis score. NSV showed a strong responsiveness to clinical change (standardized response mean values >1) and satisfactory discriminant validity. High baseline NSV (>4.6) had high predictive value (100%) with respect to erosive progression.**

Conclusion. **The proposed automated method allowed reliable quantification of NSV, which represents a promising imaging biomarker of disease activity in JIA. The automated system has the potential to improve the longitudinal assessment of JIA and to predict progressive joint destruction.**

INTRODUCTION

Juvenile idiopathic arthritis (JIA) is characterized by a chronic inflammatory process primarily targeting the synovial membrane. Persistent synovitis may lead to an increased risk of osteocartilagineous damage and functional impairment (1). The shared opinion that early suppression of inflammation is needed in order to prevent joint destruction (2,3) has increased the need of a sensitive monitoring of inflammatory changes and of prognostic markers of disease progression in order to identify patients requiring an earlier and more aggressive treatment. Contrast-enhanced magnetic resonance imaging (MRI) is capable of depicting synovial inflammation with a high degree of

Supported by the European Union (Health-e-Child Integrated Project; grant IST-2004-027749).

[1]C. Malattia, MD, PhD, A. Ravelli, MD, A. Martini, MD: Istituto Giannina Gaslini and Università di Genova, Genova, Italy; [2]M. B. Damasio, MD, S. Pederzoli, MD, C. Mattiuz, MD, S. Viola, MD, A. Buoncompagni, MD, A. Madeo, MD, M. Mazzoni, MD, G. M. Magnano, MD: Istituto Giannina Gaslini, Genova, Italy; [3]C. Basso, PhD, M. Santoro, PhD, A. Verri, PhD: Università di Genova, Genova, Italy; [4]K. Rosendahl, MD: Haukeland University Hospital and Institute of Surgical Sciences, Bergen, Norway; [5]K. Lambot-Juhan, MD: Hopital Necker Enfants Malades, Paris, France; [6]L. Tanturri de Horatio, MD: Ospedale Pediatrico Bambino Gesù, Rome, Italy.

Address correspondence to C. Malattia, MD, PhD, Pediatria II, IRCCS G. Gaslini, Largo G. Gaslini 5, 16147 Genova, Italy. E-mail: claramalattia@ospedale-gaslini.ge.it.

Submitted for publication November 11, 2011; accepted in revised form May 4, 2012.

Significance & Innovations

- Automatic magnetic resonance imaging (MRI)–determined synovial volume was valuable in assessing disease activity and treatment response, as well as predicting joint destruction in patients with juvenile idiopathic arthritis.
- The proposed MRI software, by providing an objective, reliable, and valid automatic quantification of synovial inflammation, represents a powerful research tool that may be used in clinical studies aimed to test the efficacy of new disease-modifying pharmacologic agents.
- Advances in automated data analysis programs, by allowing an objective, fast, reproducible quantitative assessment of outcome measurements, will make imaging data more clinically useful both in clinical and research settings.

resolution, allowing reliable differentiation of active inflammatory pannus from the surrounding tissue. Although the semiquantitative Outcome Measures in Rheumatology (OMERACT) rheumatoid arthritis (RA) MRI scoring system has been extensively validated in RA (4) and recently also in JIA (5), some concerns have been expressed on its relatively poor sensitivity in detecting inflammatory changes over time in RA (6), thus potentially limiting its suitability in clinical trials.

Aiming to increase sensitivity for changes, computer-based MRI quantification methods of synovial volume (SV) have been developed. The currently available computerized methods, which have proven useful in assessing disease activity and treatment response, as well as predicting joint destruction in RA (7–11) and JIA patients (12,13), are, however, based on the time-demanding manual outlining of the SV (11,14) or they rely on semiautomatic methods (15–17) based on preset enhancement thresholds, which showed poor reproducibility compared to the manual ones (7).

The purpose of the present study was to introduce a novel automated system for the MRI quantification of SV and to provide preliminary evidence of its feasibility and validity in patients with JIA.

PATIENTS AND METHODS

Seventy-eight patients with JIA, according to the International League of Associations for Rheumatology revised criteria (18), and wrist active arthritis were consecutively recruited from the study unit between March 2007 and January 2010. Excluded from the study were those patients requiring general anesthesia or with contraindication to MRI. The clinically more affected wrist was studied with MRI and radiography, coupled with a clinical examination. The following clinical assessments were recorded: count of joints with swelling, pain on motion/tenderness, and restricted motion (19); physician's global assessment of disease activity; C-reactive protein (CRP) level (nephelometry); assessment of functional ability using the Childhood Health Assessment Questionnaire (20); the Juvenile Arthritis Disease Activity Score (21); and the Juvenile Arthritis Damage Index, Articular score (22). The imaged wrist was graded on a severity scale (range 0–3) for swelling and pain, and on a limitation of motion severity scale (range 0–4) (19). Clinical measures were assessed by 2 pediatric rheumatologists (SV and AB) who were blinded to the results of imaging procedures. Patients with a 1-year followup visit were classified as improved or not improved according to the American College of Rheumatology (ACR) Pediatric (Pedi) criteria (23). The Gaslini Institutional Review Board approved the study, and informed written consent was obtained from a parent of each child.

Imaging assessment. All MRIs were performed in the same MRI unit with a 1.5T scanner (Achieva Intera; Philips Medical Systems) using a Sense Flex small coil. Details of the sequences are given in Table 1. The MR images were automatically processed to identify the voxels belonging to the inflamed synovium in the wrist joint recesses (the distal radioulnar, radiocarpal, midcarpal, and carpometacarpal joints 2–5) and tendon sheaths. The processing was performed using software developed in-house and trained on a subset of 17 MRIs (those performed at the beginning of the study) independently and manually annotated by a pediatric radiologist (MBD) and a pediatric rheumatologist (CM) with more than 5 years of experience in MRI analysis. These studies were used only in training the voxel classifier and were excluded from subsequent analysis. As previously described (24), the images were first standardized in intensity by linear normalization, followed by histogram matching (25), and, in position, by

Table 1. Imaging parameters of the MRI sequences*

Sequences	TR, msec	TE, msec/ FA, degrees	FOV, mm	Slice thickness/ gap, mm	Voxel size	Sample averages, no.	Acquisition time, min:sec
Coronal TSE T1 3-D	600	10	160	0.8	0.8 × 0.4 × 0.4	2	5 min
Coronal TSE T2 fat sat.	2,715	70	160	3/0.3	0.55 × 0.7 × 3	4	2:40
Coronal GRE 3-D fat sat. post-CM	40	7/25	160	0.8	0.8 × 0.4 × 0.4	1	4:9

* MRI = magnetic resonance imaging; TR = repetition time; TE = echo time; FA = flip angle; FOV = field of view; TSE = turbo spin-echo; 3-D = 3-dimensional; fat sat. = fat saturation; GRE = gradient echo; CM = contrast medium.

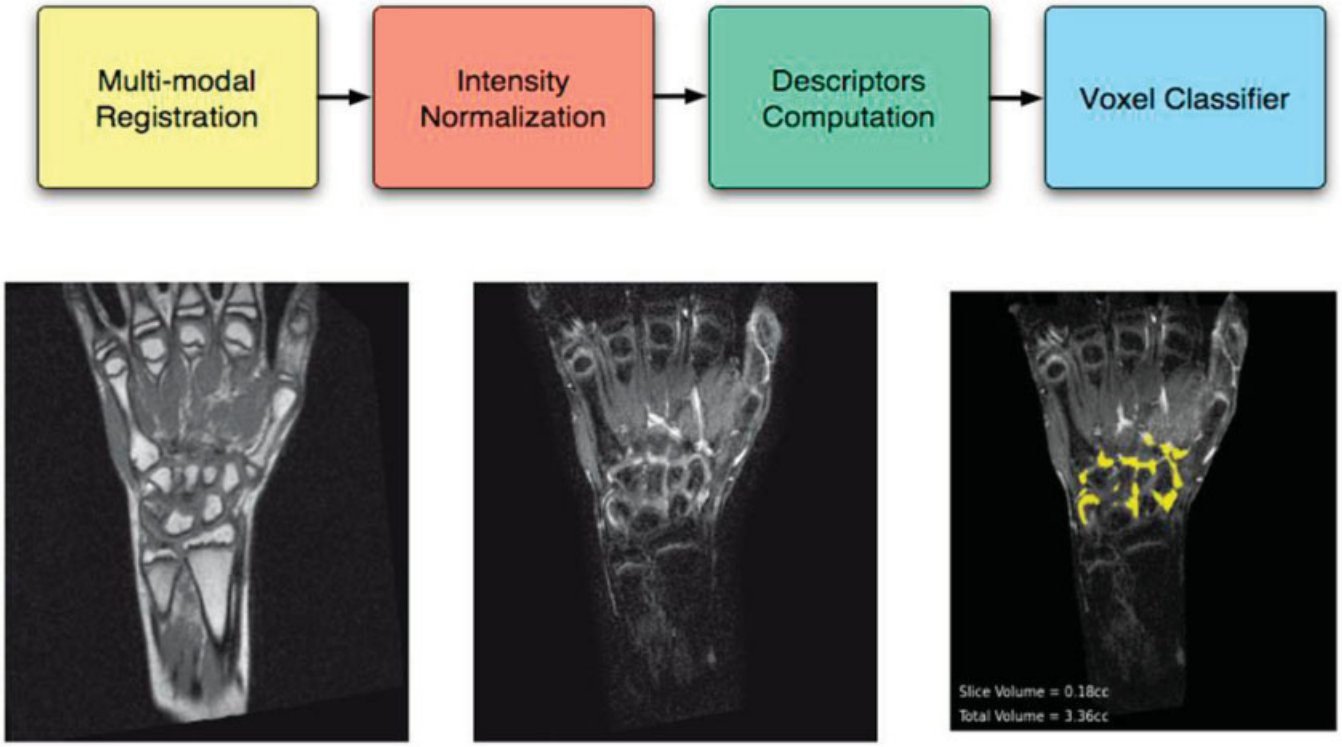

Figure 1. Scheme of the algorithm processing blocks (top) and example of input/output of the method (bottom). The input pre- and postcontrast images are first standardized in space and intensity by multimodal registration and histogram equalization. The 2 standardized images (bottom, left and middle) are then used to compute the multiparametric voxel descriptors. The descriptors are fed as input to a classifier previously trained on manually annotated data, and are used to automatically identify the voxels belonging to the inflamed synovial tissue. The same slice (bottom right) shows the detected inflammation highlighted in yellow, as well as the estimated volume in that slice and for the whole image reported in the lower left corner.

intra- and interpatient image registration based on the maximization of mutual information (26).

Multiparametric descriptors of the voxels and their neighborhoods were computed and used to classify the voxels. The full pipeline is shown in Figure 1. Each voxel descriptor was computed from pre- and postcontrast images, taking into account the intensity patterns around the voxel, as well as its position and intensity level. Such descriptors allowed us to discriminate between the voxels belonging to the inflamed synovium and those with similar high signal intensity from adjacent blood vessels, bone marrow edema, and cartilage. The classification was performed using a supervised machine learning algorithm, which returns for each voxel its likelihood of belonging to the inflamed synovium. If the likelihood is higher than a given threshold, the voxel is classified as positive. The output of the automatic process was visually verified and, when needed, the automatic output was corrected by modifying the likelihood threshold. The SV, estimated as the number of positively classified voxels multiplied by their volume, was then normalized by the patient's body surface (NSV) and used for the analysis.

The Rheumatoid Arthritis Magnetic Resonance Imaging Scoring (RAMRIS) system synovitis score (4) and the pediatric MRI bone erosion score (range 0–4) (5) were assigned to all studies in consensus by 2 experienced musculoskeletal radiologists (CM and GMM) blinded to the patient clinical status. The 1-year followup MRIs were scored without reference to baseline. Conventional radiographs were assessed by trained readers (SP and MM), according to the adapted version of the Sharp/van der Heijde score (27) and to the Poznanski score (28).

Statistical analyses. Group comparisons were performed using the Mann-Whitney U test or the Kruskal-Wallis test. A comparison of paired quantitative data was performed by Wilcoxon's test. Validation procedure included the analysis of reliability, construct validity, discriminant validity, and responsiveness to change. The reliability of our tool was tested on 15 randomly selected patients whose MRIs were independently and manually annotated by physicians (CM and MBD). The agreement between the automated and the manual NSV measurements were analyzed by computing the intraclass correlation coefficient (ICC) (29) and classifying as follows: ICC <0.4 = poor, $\geq 0.4-0.80$ = moderate, and ≥ 0.80 = good agreement. Construct validity examines whether the construct in question is related to other measures in a manner consistent with a priori prediction. Given that MRI-determined NSV should reflect disease activity, it was predicted that the correlation of its value with local disease activity parameters would be in the moderate to high range, and with global disease activity parameters would be moderate. Correlations with conventional measures of damage were predicted to be poor. All correlations were assessed using

Table 2. Baseline and followup clinical and imaging findings of the patients enrolled*

	Cross-sectional (n = 58)	Baseline (n = 36)	Followup (n = 36)	Training set (n = 17)†
Age at study visit, years	11 (8.6, 14.4)	10.7 (8.4, 13.1)	12.0 (9.5, 14.9)	9.9 (9, 15)
Disease duration, years	4.2 (1.7, 6.4)	4.2 (2.4, 5.9)	5.5 (3.4, 7.6)	3.6 (2.3, 7.6)
No. of active joints	7 (2, 17)	6.5 (2, 17)	1.5 (0, 6)	8 (1, 15)
No. of joints with LOM	4 (2, 18)	4 (2, 17)	2 (1, 6)	6 (2, 15)
VAS physician	5.9 (1.9, 8.3)	5.6 (1.7, 8.2)	0.9 (0, 2.4)	7 (3.2, 8.8)
C-HAQ score (0 = best, 3 = worst)	0.4 (0, 1.1)	0.3 (0, 0.9)	0.3 (0, 0.6)	0.7 (0, 0.8)
VAS pain, cm (0 = no pain, 10 = maximum pain)	2.5 (0.8, 5.2)	1.9 (0.1, 4.7)	0.8 (0.1, 3.1)	2 (0.1, 3.6)
Global VAS patient, cm (0 = very good, 10 = very poor)	2.4 (0.8, 4.6)	2 (0.2, 4.7)	1.1 (0.1, 4.3)	3 (0.1, 4.4)
JADI-A (range 0–72)	0.0 (0.0, 1.0)	0.0 (0.0, 2.0)	0.0 (0.0, 0.2)	0.0 (0.0, 1.0)
JADAS 71 (range 0–101)	13.9 (5.5, 28.3)	13.6 (6.2, 37.3)	5.1 (1.2, 11.5)	18 (7.8, 32)
CRP level, mg/dl (normal <0.46)	0.6 (0.46, 5.1)	0.5 (0.46, 3.4)	0.5 (0.46, 0.5)	1.8 (0.46, 5.2)
NSV	2.52 (1.74, 4.32)	3.49 (2.3, 4.79)	1.76 (0.98, 2.4)	2.87 (2.46, 4.15)
RAMRIS synovitis score	3.0 (3.0, 5.0)	3.5 (2.5, 5.5)	2.8 (1.5, 3.4)	4 (3, 5.7)
Adapted Sharp/van der Heijde score	–	18 (10.2, 26.8)	16 (11.5, 22.5)	15 (9, 17)
Poznanski score	−1.4 (−2.4, −0.4)	−1.9 (−2.6, −1.1)	−1.9 (−2.7, −0.1)	−1.9 (−2.4, −1.2)

* Values are the median (interquartile range). LOM = limitation of motion; VAS = visual analog scale; C-HAQ = Childhood Health Assessment Questionnaire; JADI = Juvenile Arthritis Damage Index-Articular; JADAS 71 = Juvenile Arthritis Disease Activity Score for 71 joints; CRP = C-reactive protein; NSV = normalized synovial volume; RAMRIS = Rheumatoid Arthritis Magnetic Resonance Imaging Scoring system.
† Reports clinical and imaging data of the first 17 patients enrolled in the study whose images were used to train the algorithm. These studies were used only in training the voxel classifier and were excluded from subsequent analysis.

Spearman's rank order correlation coefficient (r_s) (30). The responsiveness to change was assessed by computing the standardized response mean (SRM) that was calculated as the ratio between the mean and the SD of the change in NSV. The threshold levels for SRM were defined as follows: ≥0.20 = small, ≥0.50 = moderate, and ≥0.80 = strong (31). For the assessment of discriminant validity we characterized patients according to the ACR Pedi response criteria (23). Patients were divided by their maximum level of improvement into 3 mutually exclusive groups as follows: nonresponders, ACR Pedi 30 and 50 responders, and ACR Pedi 70 responders. ACR Pedi 30 and 50 responders were grouped because of their small sizes.

A receiver operating characteristic curve was computed for estimating NSV cutoff value predicting patients with erosive progression (32). MRI progression was defined as a more than 1 unit increase in 1-year MRI erosion score (33). All statistical tests were 2-sided, and *P* values less than 0.05 were considered statistically significant. Statistical analysis was performed with software developed in-house with the Python programming language (http://www.python.org) and the Scipy scientific software library (http://www.scipy.org).

RESULTS

The software for the automatic assessment of SV was tested on 61 patients; 3 patients were excluded due to a failure in the image standardization process, and in 11 patients a correction of the automatic output was applied. The NSV from 58 patients (14 boys, 44 girls) was included in validation analysis. Seventeen patients (29.3%) had systemic arthritis, 22 (37.9%) had polyarthritis (7 were positive for rheumatoid factor), and 15 (25.8%) had extended and 4 (6.9%) had persistent oligoarthritis. Nineteen patients (32.7%) were receiving disease-modifying antirheumatic drugs, and 15 (25.9%) were treated with biologic agents (8 of them with a combination of tumor necrosis factor blocker and methotrexate). Three patients (5.2%) were receiving systemic corticosteroid therapy, and 14 (24.1%) were taking nonsteroidal antiinflammatory drugs. Table 2 summarizes the results of the clinical and imaging assessment. Thirty-six of 58 patients who were enrolled during the first years of the study had a 1-year MRI followup.

Reliability. The reliability of our system was tested on 15 patients whose MRIs were manually outlined by physicians. The manual annotation took from 8–50 minutes per patient, depending on the amount of synovial membrane to be outlined. The agreement between the automated estimation of the NSV (mean 4.177, range 1.82–9.97) and the manual measurements (mean 4.098, range 1.24–10.9) was excellent (ICC 0.93, 95% confidence interval [95% CI] 0.79–0.98). Figure 2 shows "difference against mean" plots as proposed by Bland and Altman; the observations were spread homogeneously around the mean on the scatterplot. No systematic biases were observed, since the mean difference between manually outlined and automatic determined SV was low (bias −0.1; 95% limits of agreement ±1.4).

The intrareader reliability of the automated system was assessed on a subset of 15 other randomly selected examinations in which MRI scans were processed by the software on 2 different occasions. The agreement between the first reading (mean SV 5.58, range 2.45–10.99) and the second reading (mean SV 5.55, range 2.48–10.97) was excellent (ICC 0.999, 95% CI 0.999–0.999). The mean difference between the 2 sets of measurements, according to a Bland-Altman analysis, was extremely low (bias 0.03; 95% limits of agreement −0.10 to 0.16).

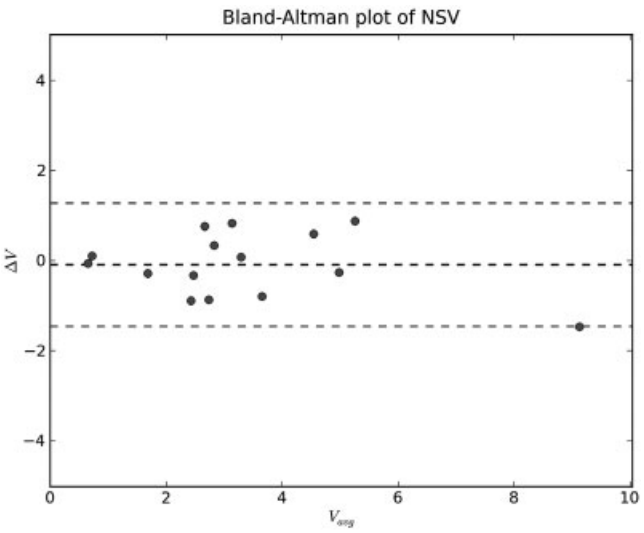

Figure 2. Bland-Altman plot of the manual and automatic measurements of the normalized synovial volume (NSV). The averages (automated + manual)/2 is the abscissa, while the difference (automated − manual NSV) is the ordinate. Broken lines show the mean difference and the 95% confidence limits of the difference.

Construct validity: correlation on cross-sectional data (n = 58). As shown in Figure 3, NSV values were significantly higher in patients with higher wrist swelling and pain scores (2–3), with respect to patients with lower swelling and pain scores (0–1; $P < 0.0005$ and $P < 0.0002$, respectively). NSV was moderately correlated with the physician's global assessment of disease activity ($r_s = 0.4$, $P < 0.002$) and with the RAMRIS synovitis score ($r_s = 0.4$, $P < 0.005$). As predicted, no correlations were found between the NSV and the conventional parameters of damage.

Sensitivity to change and discriminant validity. Median NSV values significantly decreased from baseline to 1-year MRI followup (3.49 to 1.76; $P < 0.00001$). At 1-year followup, 18 of 36 patients were improved according to the ACR Pedi criteria, while 18 were nonresponders; the frequency of ACR Pedi 30 (n = 18), Pedi 50 (n = 14), and Pedi 70 (n = 11) response was 50%, 38.9%, and 30.6%, respectively. Improved patients according to the ACR Pedi 30, 50, and 70 criteria showed a significant decrease in the NSV, resulting in the following SRM values: 1.29, 1.42, and 2.34, respectively. The SRMs of the semiquantitative RAMRIS synovitis score for each ACR category (ACR Pedi 30, 50, and 70) were 0.83, 1.0, and 1.08, respectively.

ACR Pedi 70 responders showed a significantly higher decrease in NSV compared to patients who met the ACR Pedi 30 and 50 criteria ($P < 0.02$) and compared to nonresponders ($P < 0.002$), indicating the ability of NSV to discriminate between these groups of ACR Pedi responders and between ACR Pedi 70 and nonresponders. The RAMRIS synovitis score did not discriminate among different ACR Pedi categories.

Predictive value. In patients with erosive progression (n = 20), the MRI bone erosion score significantly increased from baseline (median value 2.0) to 1-year followup (median value 7.2; $P < 0.0001$). Erosive progression as revealed by MRI was moderately correlated with baseline NSV ($r_s = 0.42$, $P < 0.02$); with the only exception of CRP ($r_s = 0.40$, $P < 0.02$), no other correlations were found either with baseline clinical measures of disease activity or with the RAMRIS synovitis score. The relationship between baseline NSV and erosive progression is shown in Figure 4. The cutoff NSV value predictive of erosive progression was 4.58. All patients with baseline NSV ≥4.58 showed erosive progression at MRI followup, indicating a 100% specificity of the baseline NSV. Conversely, 7 patients with erosive progression had a baseline NSV <4.58, indicating a sensitivity of 65%. Positive and negative predictive values were 100% and 69.6%, respectively, while the overall accuracy was 80.6%. No correlations were

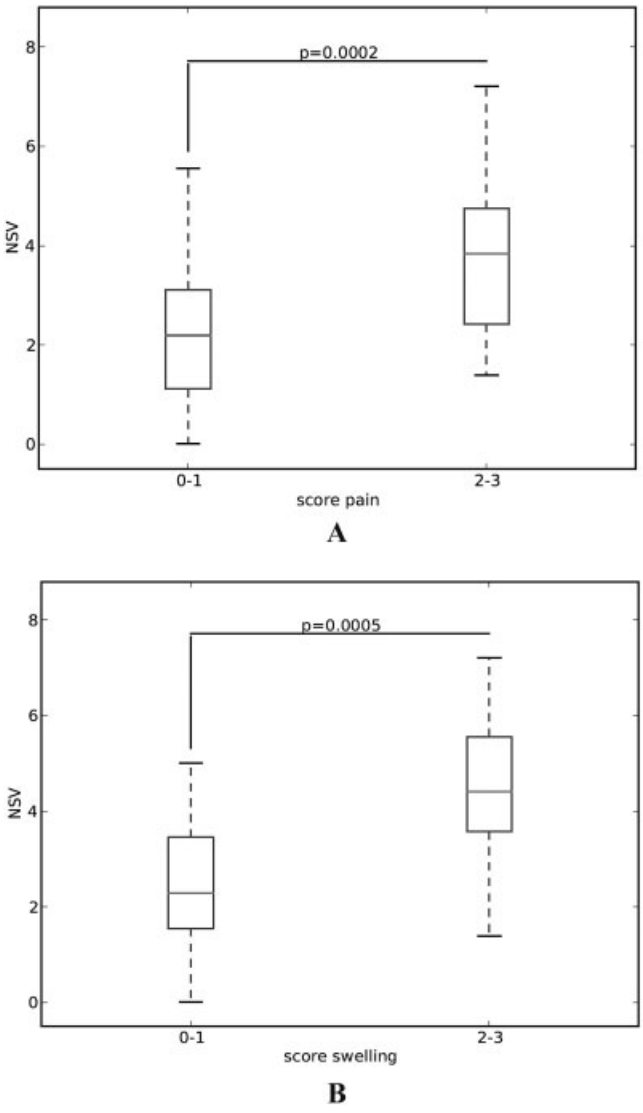

Figure 3. A, relationship between normalized synovial volume (NSV) and the severity of the wrist pain; NSV is significantly higher in patients with a higher wrist pain score (2–3) with respect to patients with lower pain score (0–1, median 3.92 versus 2.26; $P < 0.0002$). **B,** relationship between NSV and the severity of the wrist swelling; NSV is significantly higher in patients with a higher wrist swelling score (2–3) with respect to patients with lower swelling score (0–1, median 4.28 versus 2.45; $P < 0.0005$).

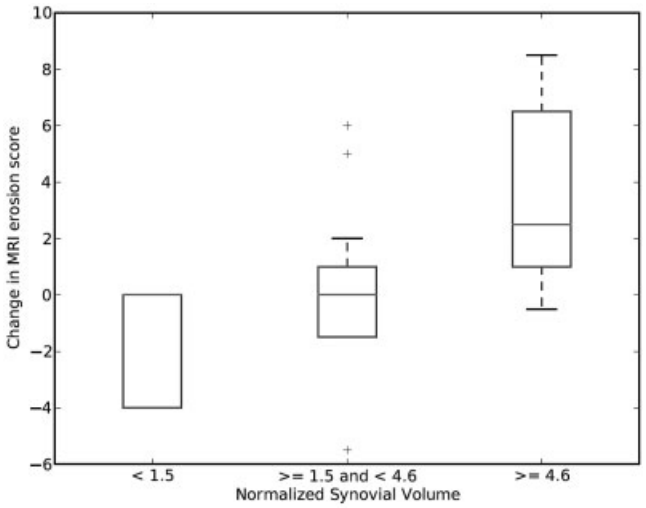

Figure 4. Relationship between baseline normalized synovial volume (NSV) and joint damage measured as 1-year magnetic resonance imaging (MRI) erosive progression. Patients were grouped in subcategories determined by the tertiles values of the distribution of the NSV values. Patients with baseline NSV >4.58 experienced a significantly higher risk of erosive progression compared to patients with baseline NSV between 1.52 and 4.58 ($P < 0.002$) and NSV <1.52 ($P < 0.02$).

found between baseline NSV and radiography bone erosion score. Nineteen of 36 patients did not show clinical signs of wrist active arthritis at the followup visit but had persistent synovitis (subclinical disease) as revealed by MRI.

DISCUSSION

Since the goal of new treatments is to obtain suppression of joint inflammation to prevent erosive damage, future outcome measures should comprise sensitive methods for monitoring joint inflammation; meanwhile, reliable prognostic markers that can separate mild from severe progressive disease are needed. The current knowledge suggests that MRI-determined SV may be useful in assessing disease activity, treatment response, and predicting joint destruction (7–13). The manual outlining of the inflamed membrane is considered the most accurate tool, even if extremely time consuming and requiring a skilled operator (6,11,14). Approaches to automated SV assessment by MRI have so far consisted of semiautomatic counting of pixels whose intensity level is above a certain threshold (15–17). The reproducibility of semiautomated measurements, however, was poorer than that obtained with manual outlining, and critically dependent on the threshold chosen (7).

We devised a novel automated method for the MRI quantification of SV and demonstrated its value as a marker of disease activity and predictor of erosive progression. The tool provides SV measurements using a novel automated segmentation program capable of automatically identifying all the voxels belonging to the inflamed synovium, while excluding those from adjacent blood vessels, bone edema, and cartilage. The advantages of this method are 2-fold. First, automating the measurement process improves the objectivity and reduces interobserver variability, as well as the time required by the operator. Second, identifying the voxels using more information such as the intensity patterns in their neighborhood or their positions, rather than just their intensity levels, allows for higher measurement accuracy. We demonstrated that the automated-determined NSV has adequate standards of validity, reliability, and feasibility, which are the components of the OMERACT filter (34). Concerning feasibility, it should be mentioned that the automated assessment of SV did not require additional sequences to the standard MRI protocol and did not increase the cost and the duration of the scan; furthermore, as mentioned above, it provided time-saving advantages. The cost related to the postprocessing is currently difficult to determine, since the software had been originally developed for research use, and it is not yet commercially available. The main problem concerning the validation of automatic-determined NSV was to find an appropriate gold standard. A strong correlation between MRI-determined SV using a manual outlining method and histologic markers of inflammation was demonstrated in RA (35), suggesting that the manual segmentation technique itself might represent such a standard (7,35). In the present study, the agreement between the computerized and manual measurements was excellent, suggesting that the automated system was reliable. In line with previous studies (8,11,12,36,37), NSV was strongly correlated with local signs of inflammation and moderately correlated with physician assessment of disease activity and with RAMRIS synovitis score, thus providing preliminary evidence for its construct validity. The lack of strong correlations with other global variables of disease activity was not surprising, given the focal nature of the MRI examination and the global nature of measures such as the active joint count and serum indicators of inflammation (5,8,11,12,38).

The automatic-determined NSV appeared to be a more responsive measure than the RAMRIS synovitis score. The responsiveness to change is a crucial property for an outcome measure, since it may reduce the number of patients to be investigated, as well as the time of exposure to the tested drug in clinical studies. The greater responsiveness of NSV may be due to the fact that the automated software provided quantification of NSV changes on a continuous scale. A higher sensitivity to longitudinal changes when a continuous measure is employed was suggested in previous studies (39). Unlike the RAMRIS synovitis score, the automatic software was able to detect significant NSV changes among different ACR categories, revealing its satisfactory discriminant validity.

In keeping with the results of previous studies (8,14,35), higher baseline NSV values were correlated with a more severe disease course in terms of structural damage progression, further suggesting that NSV may have prognostic value. Notably, no correlations with erosive progression were found either with the baseline RAMRIS synovitis score or with clinical parameters. We also provide a threshold level of MRI-determined SV that is of importance for subsequent erosive progression. Remarkably, structural damage progression was found in 100% of patients with baseline NSV higher than 4.58, but also in a portion of patients with lower NSV. The notion that mul-

tiple factors besides NSV are involved in progressive joint destruction might explain the erosive progression of these patients. Since the aim of the present study was not to identify predictors of damage, other potential markers of disease severity, such as bone marrow edema, were not investigated. A multivariate logistic regression analysis in a larger cohort of patients is therefore required to establish the independent predictive value of baseline NSV.

The well-established lower sensitivity of conventional radiography compared to MRI in the assessment of bone damage could explain the lack of correlation between baseline NSV and radiographic erosive progression (40–42). Although short-term erosion progression on MRI is highly correlated with long-term radiographic progression in RA (43), longer radiographic followup is required in order to demonstrate the predictive value of NSV in the assessment of long-term damage.

Although NSV significantly decreased from baseline to followup evaluation, only a few patients experienced the disappearance of synovitis at the 1-year MRI, hence providing a potential explanation for erosive progression in our cohort. Moreover, our results confirmed the high sensitivity of MRI in detecting subclinical synovitis, a finding that was demonstrated to be associated with structural damage progression in RA (44,45).

The lack of data from age-matched healthy controls is one of the limitations of this study. In fact, high prevalence of bony depression resembling bone erosion, as well as bone marrow edema and joint effusion, has been recently reported in healthy children (46). However, the considerable experience of our readers, with their knowledge of growth-related changes in childhood, as well as the wide spectrum of bone lesions that might be misconceived with erosion, should minimize the risk of a false-positive finding.

Although a correction of the automated output was required in approximately 20% of the patients, thereby undermining our claim that the method is fully automated, most of the cases requiring a correction were patients with low-level inflammation/remission. We argue that training the voxel classifier on a larger spectrum of disease severity, especially including patients without synovial inflammation, could significantly reduce the human intervention and increase the "ease of use of this tool," and hence its feasibility. The results of the present study may not be applicable to all JIA patients, but only to those with wrist involvement. This joint is usually affected in patients with polyarticular course (thus explaining percentage of systemic and polyarticular JIA subtype included in the present study), who are more likely to develop destructive joint damage (47). Finally, our findings are of value only for patients investigated with the present MRI protocol; therefore, the inter-MRI equipment variability is worth testing in the future, in view of the employment of this tool in multicenter clinical studies.

In conclusion, the proposed automated tool represents a promising technique to accurately and reliably assess NSV as an imaging biomarker of disease activity in JIA. If the predictive value of NSV will be confirmed in larger longitudinal studies, the automated NSV might be considered a useful marker of disease severity and employed to select patients who need more aggressive therapy.

ACKNOWLEDGMENTS

The authors wish to acknowledge the technical staff of the Radiological Department of the G. Gaslini Institute, in particular Mrs. Francesca Maiuri, Mr. Paolo Del Mirto, Mr. Stefano Franceschi, and Mr. Marco Ciccone, who supervised the MRI scans.

AUTHOR CONTRIBUTIONS

All authors were involved in drafting the article or revising it critically for important intellectual content, and all authors approved the final version to be submitted for publication. Dr. Malattia had full access to all of the data in the study and takes responsibility for the integrity of the data and the accuracy of the data analysis.

Study conception and design. Malattia, Damasio, Basso, Verri, Pederzoli, Tanturri de Horatio, Magnano, Ravelli, Martini.

Acquisition of data. Malattia, Damasio, Basso, Santoro, Pederzoli, Mattiuz, Viola, Buoncompagni, Madeo, Mazzoni.

Analysis and interpretation of data. Malattia, Damasio, Basso, Pederzoli, Rosendahl, Lambot-Juhan, Ravelli, Martini.

REFERENCES

1. Ravelli A, Martini A. Juvenile idiopathic arthritis. Lancet 2007;369:767–78.
2. Martini A, Lovell DJ. Juvenile idiopathic arthritis: state of the art and future perspectives. Ann Rheum Dis 2010;69:1260–3.
3. Breedveld F. The value of early intervention in RA: a window of opportunity. Clin Rheumatol 2011;30 Suppl 1:S33–9.
4. Ostergaard M, Peterfy C, Conaghan P, McQueen F, Bird P, Ejbjerg B, et al. OMERACT Rheumatoid Arthritis Magnetic Resonance Imaging Studies. Core set of MRI acquisitions, joint pathology definitions, and the OMERACT RA-MRI scoring system. J Rheumatol 2003;30:1385–6.
5. Malattia C, Damasio MB, Pistorio A, Ioseliani M, Vilca I, Valle M, et al. Development and preliminary validation of a paediatric-targeted MRI scoring system for the assessment of disease activity and damage in juvenile idiopathic arthritis. Ann Rheum Dis 2010;70:440–6.
6. Hodgson RJ, O'Connor P, Moots R. MRI of rheumatoid arthritis–image quantitation for the assessment of disease activity, progression and response to therapy. Rheumatology (Oxford) 2008;47:13–21.
7. Ostergaard M. Different approaches to synovial membrane volume determination by magnetic resonance imaging: manual versus automated segmentation. Br J Rheumatol 1997;36:1166–77.
8. Ostergaard M, Hansen M, Stoltenberg M, Gideon P, Klarlund M, Jensen KE, et al. Magnetic resonance imaging–determined synovial membrane volume as a marker of disease activity and a predictor of progressive joint destruction in the wrists of patients with rheumatoid arthritis. Arthritis Rheum 1999;42:918–29.
9. Zikou AK, Argyropoulou MI, Voulgari PV, Xydis VG, Nikas SN, Efremidis SC, et al. Magnetic resonance imaging quantification of hand synovitis in patients with rheumatoid arthritis treated with adalimumab. J Rheumatol 2006;33:219–23.
10. Sugimoto H, Takeda A, Kano S. Assessment of disease activity in rheumatoid arthritis using magnetic resonance imaging: quantification of pannus volume in hands. Br J Rheumatol 1998;37:854–61.
11. Bird P, Lassere M, Shnier R, Edmonds J. Computerized measurement of magnetic resonance imaging erosion volumes in patients with rheumatoid arthritis: a comparison with existing magnetic resonance imaging scoring systems and standard clinical outcome measures. Arthritis Rheum 2003;48:614–24.

12. Graham TB, Laor T, Dardzinski BJ. Quantitative magnetic resonance imaging of the hands and wrists of children with juvenile rheumatoid arthritis. J Rheumatol 2005;32:1811–20.
13. Gylys-Morin VM, Graham TB, Blebea JS, Dardzinski BJ, Laor T, Johnson ND, et al. Knee in early juvenile rheumatoid arthritis: MR imaging findings. Radiology 2001;220:696–706.
14. Savnik A, Bliddal H, Nyengaard J, Thomsen HS. MRI of the arthritic finger joints: synovial membrane volume determination, a manual versus a stereologic method. Eur Radiol 2002; 12:94–8.
15. Tam LS, Griffith J, Yu AB, Li TK, Li EK. Rapid improvement in rheumatoid arthritis patients on combination of methotrexate and infliximab: clinical and magnetic resonance imaging evaluation. Clin Rheumatol 2007;26:941–6.
16. Palmer WE, Rosenthal DI, Schoenberg OI, Fischman AJ, Simon LS, Rubin RH, et al. Quantification of inflammation in the wrist with gadolinium-enhanced MR imaging and PET with 2-(F-18)-fluoro-2-deoxy-D-glucose. Radiology 1995;196: 647–55.
17. Fritz J, Galeczko EK, Schwenzer N, Fenchel M, Claussen CD, Carrino JA, et al. Longitudinal changes in rheumatoid arthritis after rituximab administration assessed by quantitative and dynamic contrast-enhanced 3-T MR imaging: preliminary findings. Eur Radiol 2009;19:2217–24.
18. Petty RE, Southwood TR, Manners P, Baum J, Glass DN, Goldenberg J, et al. International League of Associations for Rheumatology classification of juvenile idiopathic arthritis: second revision, Edmonton 2001. J Rheumatol 2004;31: 390–2.
19. Giannini EH, Brewer EJ Jr. Standard methodology for Segment I, II, and III Pediatric Rheumatology Collaborative Study Group studies. II. Analysis and presentation of data. J Rheumatol 1982;9:114–22.
20. Ruperto N, Ravelli A, Pistorio A, Malattia C, Viola S, Cavuto S, et al. The Italian version of the Childhood Health Assessment Questionnaire (CHAQ) and the Child Health Questionnaire (CHQ). Clin Exp Rheumatol 2001;Suppl 23:S91–5.
21. Consolaro A, Ruperto N, Bazso A, Pistorio A, Magni-Manzoni S, Filocamo G, et al, and the Paediatric Rheumatology International Trials Organisation. Development and validation of a composite disease activity score for juvenile idiopathic arthritis. Arthritis Rheum 2009;61:658–66.
22. Viola S, Felici E, Magni-Manzoni S, Pistorio A, Buoncompagni A, Ruperto N, et al. Development and validation of a clinical index for assessment of long-term damage in juvenile idiopathic arthritis. Arthritis Rheum 2005;52:2092–102.
23. Giannini EH, Ruperto N, Ravelli A, Lovell DJ, Felson DT, Martini A. Preliminary definition of improvement in juvenile arthritis. Arthritis Rheum 1997;40:1202–9.
24. Basso C, Santoro M, Verri A, Esposito M. Segmentation of inflamed synovia in multi-modal 3D MRI. Proceedings of IEEE International Symposium on Biomedical Imaging: from Nano to Macro. Piscataway (NJ): IEEE Press; 2009 p. 229–32.
25. Gonzalez R, Woods R. Digital image processing. 3rd ed. Upper Saddle River (NJ): Pearson Education; 2008.
26. Mattes D, Haynor D, Vesselle H, Lewellen T, Eubank W. PET-CT image registration in the chest using free-form deformations. IEEE Trans Med Imaging 2003;22:120–8.
27. Ravelli A, Ioseliani M, Norambuena X, Sato J, Pistorio A, Rossi F, et al. Adapted versions of the Sharp/van der Heijde score are reliable and valid for assessment of radiographic progression in juvenile idiopathic arthritis. Arthritis Rheum 2007;56:3087–95.
28. Poznanski AK, Hernandez RJ, Guire KE, Bereza UL, Garn SM. Carpal length in children: a useful measurement in the diagnosis of rheumatoid arthritis and some congenital malformation syndromes. Radiology 1978;129:661–8.
29. Deyo RA, Diehr P, Patrick DL. Reproducibility and responsiveness of health status measures: statistics and strategies for evaluation. Control Clin Trials 1991;12:142–58S.
30. Swinscow TD. Statistics at square one. 9th ed. Campbell MJ, editor. Southampton: BMJ Publishing; 1997. p. 78.
31. Liang MH, Larson MG, Cullen KE, Schwartz JA. Comparative measurement efficiency and sensitivity of five health status instruments for arthritis research. Arthritis Rheum 1985;28: 542–7.
32. Obuchowski NA. Receiver operating characteristic curves and their use in radiology. Radiology 2003;229:3–8.
33. Boyesen P, Haavardsholm EA, van der Heijde D, Ostergaard M, Hammer HB, Sesseng S, et al. Prediction of MRI erosive progression: a comparison of modern imaging modalities in early rheumatoid arthritis patients. Ann Rheum Dis 2011;70: 176–9.
34. Boers M, Brooks P, Strand V, Strand CV, Tugwell P. The OMERACT filter for outcome measures in rheumatology. J Rheumatol 1998;25:198–9.
35. Ostergaard M, Stoltenberg M, Lovgreen-Nielsen P, Volck B, Jensen CH, Lorenzen I. Magnetic resonance imaging–determined synovial membrane and joint effusion volumes in rheumatoid arthritis and osteoarthritis: comparison with the macroscopic and microscopic appearance of the synovium. Arthritis Rheum 1997;40:1856–67.
36. Ostergaard M, Gideon P, Henriksen O, Lorenzen I. Synovial volume: a marker of disease severity in rheumatoid arthritis? Quantification by MRI. Scand J Rheumatol 1994;23:197–202.
37. Ostergaard M, Hansen M, Stoltenberg M, Lorenzen I. Quantitative assessment of the synovial membrane in the rheumatoid wrist: an easily obtained MRI score reflects the synovial volume. Br J Rheumatol 1996;35:965–71.
38. Backhaus M, Kamradt T, Sandrock D, Loreck D, Fritz J, Wolf KJ, et al. Arthritis of the finger joints: a comprehensive approach comparing conventional radiography, scintigraphy, ultrasound, and contrast-enhanced magnetic resonance imaging. Arthritis Rheum 1999;42:1232–45.
39. Neumann G, dePablo P, Finckh A, Chibnik LB, Wolfe F, Duryea J. Patient repositioning reproducibility of joint space width measurements on hand radiographs. Arthritis Care Res (Hoboken) 2011;63:203–7.
40. McQueen FM, Stewart N, Crabbe J, Robinson E, Yeoman S, Tan PL, et al. Magnetic resonance imaging of the wrist in early rheumatoid arthritis reveals a high prevalence of erosions at four months after symptom onset. Ann Rheum Dis 1998;57: 350–6.
41. Malattia C, Damasio MB, Magnaguagno F, Pistorio A, Valle M, Martinoli C, et al. Magnetic resonance imaging, ultrasonography, and conventional radiography in the assessment of bone erosions in juvenile idiopathic arthritis. Arthritis Rheum 2008;59:1764–72.
42. Peterfy CG. MRI of the wrist in early rheumatoid arthritis. Ann Rheum Dis 2004;63:473–7.
43. McQueen FM, Benton N, Crabbe J, Robinson E, Yeoman S, McLean L, et al. What is the fate of erosions in early rheumatoid arthritis? Tracking individual lesions using x rays and magnetic resonance imaging over the first two years of disease. Ann Rheum Dis 2001;60:859–68.
44. Brown AK, Conaghan PG, Karim Z, Quinn MA, Ikeda K, Peterfy CG, et al. An explanation for the apparent dissociation between clinical remission and continued structural deterioration in rheumatoid arthritis. Arthritis Rheum 2008;58: 2958–67.
45. McQueen FM, Stewart N, Crabbe J, Robinson E, Yeoman S, Tan PL, et al. Magnetic resonance imaging of the wrist in early rheumatoid arthritis reveals progression of erosions despite clinical improvement. Ann Rheum Dis 1999;58:156–63.
46. Muller LS, Avenarius D, Damasio B, Eldevik OP, Malattia C, Lambot-Juhan K, et al. The paediatric wrist revisited: redefining MR findings in healthy children. Ann Rheum Dis 2011; 70:605–10.
47. Magni-Manzoni S, Rossi F, Pistorio A, Temporini F, Viola S, Beluffi G, et al. Prognostic factors for radiographic progression, radiographic damage, and disability in juvenile idiopathic arthritis. Arthritis Rheum 2003;48:3509–17.